Steady-state preparation of long-lived nuclear spin singlet pairs at room temperature

Q. Chen, I. Schwarz, and M. B. Plenio

Institut für Theoretische Physik, Albert-Einstein-Allee 11, Universität Ulm, 89069 Ulm, Germany

(Received 13 March 2017; revised manuscript received 5 June 2017; published 21 June 2017)

The coherent high-fidelity generation of nuclear spins in long-lived singlet states, which may find application as quantum memory or sensor, represents a considerable experimental challenge. Here, we propose a dissipative scheme that achieves the preparation of pairs of nuclear spins in long-lived singlet states by a protocol that combines the interaction between the nuclei and a periodically reset electron spin of an nirogen-vacancy center with local radio-frequency control of the nuclear spins. The final state of this protocol is independent of the initial preparation of the nuclei, is robust to external field fluctuations, and can be operated at room temperature. We show that a high-fidelity singlet pair of a ^{13}C dimer in a nuclear bath in diamond can be generated under realistic experimental conditions.

DOI: 10.1103/PhysRevB.95.224105

I. INTRODUCTION

The preparation of nuclear spins in singlet states is attracting increasing attention due to their weak coupling to several environmental relaxation processes, especially for closely spaced nuclei when their interaction with their environment is symmetric to a very good approximation and transitions between the singlet and triplet states are suppressed. As a consequence, singlet states exhibit superior stability, which makes them promising candidates for storing nuclear hyperpolarization even beyond their relaxation time T_1 [1,2]. Nuclear spin-singlet states offer a broad range of applications in medicine, materials science, biology, and chemistry. They are used as a resource for spectroscopic interrogation of couplings within many-spin system [3,4], the monitoring of protein conformational changes [5], the probing of slow diffusion of biomolecules [6], or as quantum memories [7]. However, the key strength of nuclear singlets, namely their weak interaction with their environment due to the antisymmetry of the singlet state, is also their weakness, as it makes the high-fidelity singlet-state preparation and their manipulation a challenge [8,9].

The nitrogen-vacancy (NV) defect center in diamond which has been studied extensively over the past decade for precision sensing and quantum information processes (QIP) offers new perspectives here [10]. The NV center with its surrounding nuclei forms a natural hybrid quantum register [11,12] in which electron spins are used for fast high-fidelity control and readout, and proximal nuclear spins can be controlled and used as memories due to their ultralong coherence time. Furthermore, NV centers are excellent hyperpolarization agents to polarize nearby nuclear spins at ambient condition [13–15], which gives rise to several orders of enhancement of nuclear magnetic resonance (NMR) signals.

In these room-temperature applications of the NV center, however, relaxation processes of the NV center, which induce decoherence on both the NV and the surrounding nuclear spins, are a major obstacle for the high-fidelity preparation of entangled target states [16]. However, it has been recognized early that dissipation can also be a resource that enables entangled state preparation [17,18]. In recent years, theoretical protocols that design dissipative processes has been focused on the creation of entanglement between atoms, ions, and spins [19–24], the stabilization of quantum gates [25,26] and dissipative entanglement generation have been realized experimentally in atomic ensembles [27], ion traps [28], and superconducting qubits [29]. We stress that these results have been obtained in systems that are operating under cryogenic conditions and/or vacuum conditions.

The subject of this work is a proposal for a solid-state-based system that can achieve singlet-state generation under ambient conditions in a spin bath in which all spins are coupled to an NV electron spin in diamond. Our method includes two important features. First, the frequent resets of the NV stabilizes it in a particular state and provides a tunable artificial reservoir. Second, the coherent local control of nuclear spins by radio-frequency (rf) fields with imbalanced detunings to the two nuclear Larmor frequencies, ensures that the steady singlet state of the nuclei is unique. An important merit of dissipative state preparation is its resilience to errors due to imperfect state initialization and fluctuation of the driving fields. Our method can be applied to interacting or non-interacting nuclear spins which have similar magnitude couplings to the NV. Additionally, high-fidelity singlet pairs of a ^{13}C dimer in a nuclear bath in diamond can be generated with the realistic parameters. The so generated spin singlet state exhibits a lifetime that extends well beyond the T_1-limit of the electron spins.

II. THE MODEL

We consider an NV center and two nearby ^{13}C spins with gyromagnetic ratio γ_n, as shown in Fig. 1. Their interaction can be described by the dipole-dipole term $H_{\text{int}} = S_z \cdot \vec{A}_i \cdot \vec{I}_i$, where $\vec{A} = (a_{\parallel_i}, a_{\perp_i})$ is the hyperfine vector, with $a_{\parallel_i}$ and $a_{\perp_i}$ denoting the related coupling components parallel and perpendicular to the nuclear spin quantization axes (see more details in Appendix A), and nonsecular terms are neglected due to the energy mismatch of the two spins. In an external magnetic field B_0 (i.e., $|B_0| = 100$G), the effective Lamor frequency of nuclear spin is $\gamma_n|B_{\text{eff}}| = |\gamma_n B_0 + \frac{a_{\parallel i}}{2}|$. A microwave (MW) field (Rabi frequency Ω_{mw} and frequency ω_{mw}) and a rf field (Rabi frequency Ω_{rf} and frequency ω_{rf}) are applied to the NV and the nuclear spins, respectively. In a suitable interaction picture we can rewrite the effective Hamiltonian of the NV spin as $H_{\text{NV}} = \Omega_{\text{mw}}\sigma_z$, where the microwave is resonant with the $|m_s = 0\rangle \leftrightarrow |m_s = -1\rangle$ transition, and the microwave dressed states $\{|+_x\rangle = \frac{1}{\sqrt{2}}(|0\rangle + |-1\rangle), |-_x\rangle = \frac{1}{\sqrt{2}}(|0\rangle - |-1\rangle)\}$

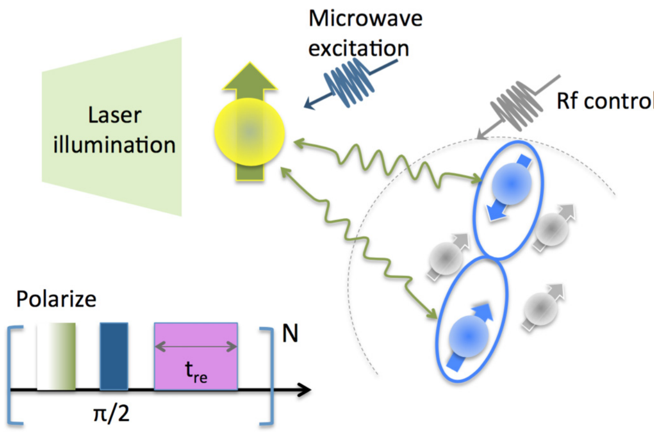

FIG. 1. A nuclear singlet pair (blue circles) is generated by using frequent resets of the NV spin and local radio-frequency (rf) control of nuclear spins. The NV spin is initialized to the $m_s = 0$ state by green laser illumination and transferred to state $|-_x\rangle = (|m_s = 0\rangle - |m_s = -1\rangle)/\sqrt{2}$ by using a microwave-$\pi/2$ pulse. The electron spin is reinitialized every $t_{\rm re}$ and MW field is applied continuously. A unique steady state of the system is obtained by suitably chosen rf driving on the nuclear spins.

define $\sigma_z = \frac{1}{2}(|+_x\rangle\langle+_x| - |-_x\rangle\langle-_x|)$. Working in a rotating frame with respect to $H_0 = \Omega_{\rm mw}\sigma_z + \sum_{i=1}^{2}\omega_{\rm rf} I_i^z$ and by using a rotating wave approximation, we find the simplified Hamiltonian (details are included in Appendix A),

$$H''_{\rm tot} = \sum_{i=1,2} \Delta_i I_i^z + \Omega_{\rm rf} I_i^x + \frac{a_{\perp i}}{4}(\sigma_+ I_i^- + {\rm H.c.}), \quad (1)$$

with $\Delta_i = \gamma_n B_0 + \frac{a_{\parallel i}}{2} - \omega_{\rm rf}$ and $\omega_{\rm rf} = \Omega_{\rm mw}$.

We follow the basic cooling cycles for nuclear spin polarization [30,31], namely an iteration between evolution according to Hamiltonian Eq. (1) followed by reinitialization of the electron spin to $|-_x\rangle$. The nuclei effectively "see" a large polarization reservoir of the periodically reset of electron spin, and the density matrix of the system evolves according to

$$\rho_n \to \cdots U_t {\rm Tr}_e[U_t(\rho_n \otimes |-_x\rangle\langle-_x|)U_t^\dagger] \otimes |-_x\rangle\langle-_x|U_t^\dagger \cdots$$

in which $U_t = \exp(-iH''_{\rm tot}t)$ is the time evolution operator, ${\rm Tr}_e$ presents the trace over the electron and ρ_n is the density matrix of nuclear spins in the system. In order to allow for a perturbative treatment, we consider short times between the NV resets ($t = t_{\rm re} < 1/\sqrt{\sum_i a_{\perp i}^2}$) we can expand the time evolution operators to second order and eliminate electronic degrees of freedom by a partial trace. The periodic resets introduce an effective relaxation mechanism and the effective relaxation of the NV spin is given by the life time $T_{1\rho}$ and the reset time $t_{\rm re}$ ($\Gamma_N = 1/T_{1\rho} + 1/t_{\rm re}$). Additionally, frequent resets with $t_{\rm re} \ll T_{1\rho}$ ensures that the electron spin stays close to the reset state $|-_x\rangle$ and $\Gamma_N \approx 1/t_{\rm re}$.

By adiabatic elimination of the NV spin (see Appendix B), the reduced density operator of the nuclear spin subsystem is governed by the master equation,

$$\frac{d}{dt}\rho_n = -i[H_T,\rho_n] + \sum_{i=1,2}\mathcal{D}[M_i]\rho_n + \mathcal{D}[L]\rho_n, \quad (2)$$

in which $\mathcal{D}[c]\rho = c\rho c^\dagger - \frac{1}{2}\{c^\dagger c,\rho\}$, $M_i = \sqrt{\Gamma_i} I_i^-$ with Γ_i the dephasing rate of the nuclear spins and $L = \sum_i \alpha_i I_i^-$ with $\alpha_j = \frac{\sqrt{\Gamma_N} a_{\perp j}/4}{-\Delta_j + i\Gamma_N/2}$. Here, the effective dissipation item $\mathcal{D}[L]\rho_n$ is due to the dissipation induced by the NV resets in combination with the interaction between the electron and nuclear spins [last term in Eq. (1)], leaving the local nuclear dynamics described by the Hamiltonian

$$H_T = \sum_{i=1,2} \Omega_{\rm rf} I_i^x + \Delta_i I_i^z. \quad (3)$$

Without the applied rf field $\Omega_{\rm rf} = 0$ and $\Delta_1 = \Delta_2$, the readily obtained master equation represents the basic cooling scheme for nuclear spin polarization. This scheme has two decoupled nuclear spin states, the fully polarized state $|\downarrow_1\downarrow_2\rangle$, as well as, for equally strong coupled spins, the dark state $|S\rangle = \frac{1}{\sqrt{2}}(|\uparrow_1\downarrow_2\rangle - |\downarrow_1\uparrow_2\rangle)$. As a result, the stationary state of the nuclear spins will be a mixture of these two states, which is neither fully polarized nor fully entangled. Our goal is the preparation of a maximally entangled singlet state. In the following, we show how local rf control can remove the fully polarization state of the nuclear spins from the manifold of stationary states such that the dynamics of the nuclear spins then converges to a singlet state.

III. SINGLET PAIR GENERATION FOR NONINTERACTING SPINS

For two nuclei that couple equally to the NV, i.e., $a_{\perp_1} = a_{\perp_2}$, and the choice $\Delta_1 = -\Delta_2$ for the rf field, the unique steady state of the system is given by the Hamiltonian H_T and dissipation part L,

$$|\psi_{\rm ss}\rangle = N_c(\sqrt{2}\Delta_1|\downarrow_1\downarrow_2\rangle - \Omega_{\rm rf}|S\rangle), \quad (4)$$

with the normalization coefficient $N_c = \frac{1}{\sqrt{2\Delta_1^2+\Omega_{\rm rf}^2}}$. It is an eigenstate to eigenvalue 0 of both, the effective Hamiltonian H_T and the Lindblad operator L. Notice that when there is no detuning, i.e., $\Delta_1 = \Delta_2$, the system is decomposable and the steady state is not unique. However, a small imbalance in the detuning between the two nuclear spins, i.e., $\Delta_1 = -\Delta_2$, breaks the symmetry and leads to $|\psi_{\rm ss}\rangle$ being the unique steady state. We use the logarithmic negativity (LN) [32,33] to measure the entanglement, ${\rm LN}(\rho_{\rm ss}) = \log_2(1 + \frac{\Omega_{\rm rf}\sqrt{2\Delta_1^2+\Omega_{\rm rf}^2}}{2\Delta_1^2+\Omega_{\rm rf}^2})$. Therefore, in the limit $\Omega_{\rm rf} \gg |\Delta|$ ($\Delta = |\Delta_1 - \Delta_2|/2$), one can have ${\rm LN} \to 1$, which shows that the steady state of the system will achieve the singlet state $|S\rangle$ independent of the initial state.

Figure 2(a) shows the result of a numerical simulation using the original full Hamiltonian Eq. (1) and periodic NV resets. The results which show near perfect singlet generation are well approximated by the effective master equation Eq. (2). Even for imperfect matched detuning ($\delta\Delta = \Delta_1 + \Delta_2 \neq 0$) and an asymmetry of the couplings ($\delta a = a_{\perp_1} - a_{\perp_2} \neq 0$) high fidelity is maintained with $\Omega_{\rm rf} = 8\Delta$ [see Fig. 2(b)]. Furthermore, our simulations show that the singlet pair generation is also robust to imperfections in the reinitialization of the NV. A reset fidelity of 96% polarization for the electron spin (achieved by current experimental technology [34]) suffices to provide a singlet state with ${\rm LN} = 0.97$.

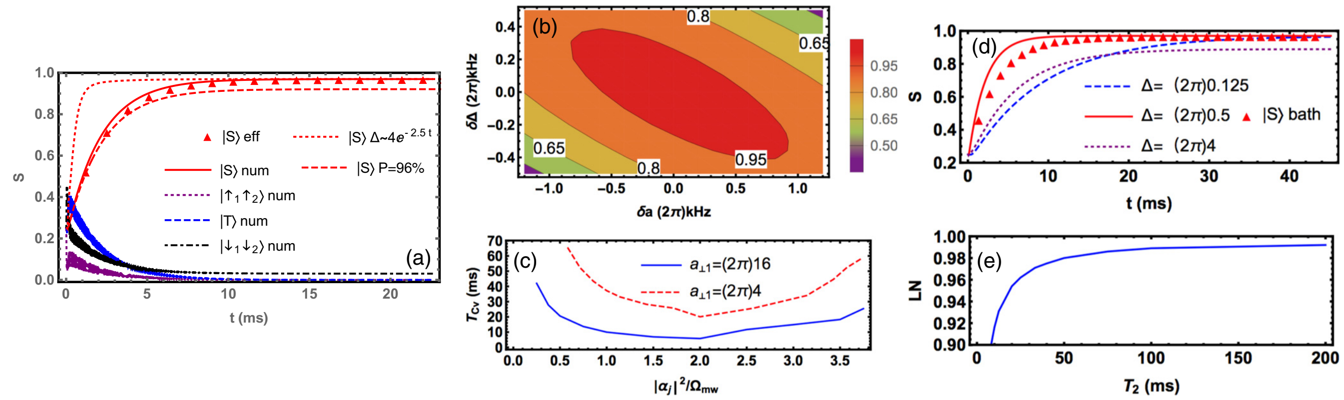

FIG. 2. (a) The population evolutions of the singlet and three triplet states $\{|S\rangle = \frac{1}{\sqrt{2}}(|\uparrow_1\downarrow_2\rangle - |\downarrow_1\uparrow_2\rangle), |\uparrow_1\uparrow_2\rangle, |\downarrow_1\downarrow_2\rangle, |T\rangle = \frac{1}{\sqrt{2}}(|\uparrow_1\downarrow_2\rangle + |\downarrow_1\uparrow_2\rangle)\}$ as a function of time for a fully mixture state $\rho_n = I/4$ initially. The NV spin is reset every 40 μs ($T_{1\rho} = 2$ ms) providing the tunable artificial reservoir. The two nuclei are coupled to the NV center (distance $\sim$1.2 nm) as $(a_{\parallel_1}, a_{\perp_1}) = (2\pi)(2,16)$ kHz and $(a_{\parallel_2}, a_{\perp_2}) = (2\pi)(4,16)$ kHz, which results in $\Delta = (2\pi)0.5$ kHz, $\Omega_{\rm rf} = 8\Delta$. Exponential detuning accelerates the convergence time (red dotted line) and imperfect reset of NV center also gives high LN ~ 0.96 of singlet state generation (red dashed line). Take the parameters as shown by the red solid line in (a) as an example to demonstrate the effect of imperfections: (b) the LN is given due to imperfections of the detunings and couplings with the same Δ and evolution time $t = 20$ ms. (c) The convergence time $T_{\rm Cv}$ for achieving LN $= 0.97$ vs. the ratio $|\alpha|_j^2/\Omega_{\rm mw}$ for different perpendicular couplings (Here we adjust $t_{\rm re}$ as an example and $|\alpha|_j^2 \approx a_{\perp j}^2 t_{\rm re}/4$). (d) Optimized singlet state generation of different detunings with $\Omega_{\rm rf} = 8\Delta$ and $|\alpha|_j^2/\Omega_{\rm rf} = 2$. As a comparison, we consider a small nuclear bath (red triangles), in which coupling strengths of three different nuclear spins are $(a_{\parallel_3}, a_{\perp_3}) = (2\pi)(13,8)$ kHz, $(a_{\parallel_4}, a_{\perp_4}) = (2\pi)(-11,3)$ kHz and $(a_{\parallel_5}, a_{\perp_5}) = (2\pi)(20,4)$ kHz. And (e) with $\Delta/\Omega_{\rm rf} = \sqrt{k_j/2}$, the optimized fidelity as a function of T_2 of nuclear spins.

Another important factor for dissipative entanglement generation is the convergence time $T_{\rm Cv}$ of the scheme. $T_{\rm Cv}$ is limited by the effective dissipation rate $|\alpha_i|^2$ ($|\alpha_1| \approx |\alpha_2|$) and the strength of $\Omega_{\rm rf}$ of the local rf control and the detuning Δ via the ratios $\Delta/\Omega_{\rm rf}$ and $|\alpha_i|^2/\Omega_{\rm rf}$. Notice that $\Delta/\Omega_{\rm rf}$ also controls the singlet generation fidelity and we use $\Delta/\Omega_{\rm rf} = 1/8$ to ensure high fidelity, which in turn induces a relatively long $T_{\rm Cv}$. For a given Δ, we find that the optimal convergence time is achieved for $|\alpha|^2/\Omega_{\rm rf} = 2$; [see Fig. 2(c)]. Additionally, the convergence may be accelerated by using an adiabatic change of the imbalance of the detuning Δ over time. The choice $\Delta = (2\pi)4e^{-2.5t}$ kHz yields the dotted red line in Fig. 2(a), which favors rapid approach to the target.

The singlet state preparation can be controlled by using the weak external magnetic field (i.e., $|B_0| = 100$G). Choosing two nuclei with similar couplings to the NV we can adjust the external magnetic field direction to obtain the same perpendicular coupling components and a difference between parallel components. As the detuning Δ is induced by the parallel components, choosing the NV reset time $t_{\rm re}$ and Rabi frequency $\Omega_{\rm rf}$ appropriately achieves high fidelity of singlet pair generation and relatively short convergence time. As shown in Fig. 2(d), a singlet pair is generated with high fidelity for a large range $(2\pi)0.125$ kHz $< \Delta < (2\pi)4$ kHz. Additionally, Δ is also tunable via a magnetic field gradient [35], which makes the adiabatic change of the detuning imbalance Δ possible [35]. Therefore, it is not difficult to find two nuclear spins matching the requirements for high-fidelity generation of a nuclear singlet pair.

So far we have not considered the effect of environmental noise on the nuclei. In order to model a more realistic situation, we include a small nuclear spin bath surrounding our nuclear spins pair. In Fig. 2(d), we see the impact of such a spin bath by comparing the red curve (noise free) and the red triangles (with spin bath). Notice that the other spins are unaffected by our singlet generation protocol because $|\Delta_i - \Delta| \gg 0$ and $|a_{\parallel_i} - a_{\parallel_1}| \gg 0$ and $t_{\rm re}$ is chosen such that the perturbative treatment is valid. The intrinsic decoherence of nuclear spins can be neglected when the coherence time ($T_2 > 500$ ms [36] for ^{13}C spins in diamond under ambient conditions) exceeds $T_{\rm Cv}$. For a very noisy environment, e.g., nuclear spins in a molecule on the NV surface the singlet fidelity will be adversely affected. One way to eliminate the influence of intrinsic dissipation is by increasing the engineered correlated decay α_j, which is limited by the small coupling between the NV and nuclear spins. In order to get the steady state of a two-qubit system, one can solve the system of $d^2 - 1 = 15$ differential equations for the elements of the stabilized density matrix or equivalent Bloch vector [37]. The solution is an eighth-order polynomial in which the LN can be maximized. Therefore, one can optimize the dynamics by using the first-order perturbation in the small parameter $k_j = \sqrt{\Gamma_j}/\alpha_j$, and the LN is maximized by $\Delta/\Omega_{\rm rf} = \sqrt{k_j/2}$. We show the optimized LN in Fig. 2(e). Additionally, the rate of convergence can be accelerated by starting with a large initial detuning and decrease it to the optimal value.

IV. SINGLET PAIR GENERATION FOR INTERACTING SPINS IN A DIMER

If one intends to generate a singlet state of two interacting spins in a dimer, the dipole-dipole interaction is not negligible and the local dynamics is given by

$$H'_T = \sum_{i=1,2} \Omega_{\rm rf} I_i^x + \Delta_i I_i^z + g_{12}\left[I_1^z I_2^z - \frac{1}{2}\left(I_1^x I_2^x + I_1^y I_2^y\right)\right],$$

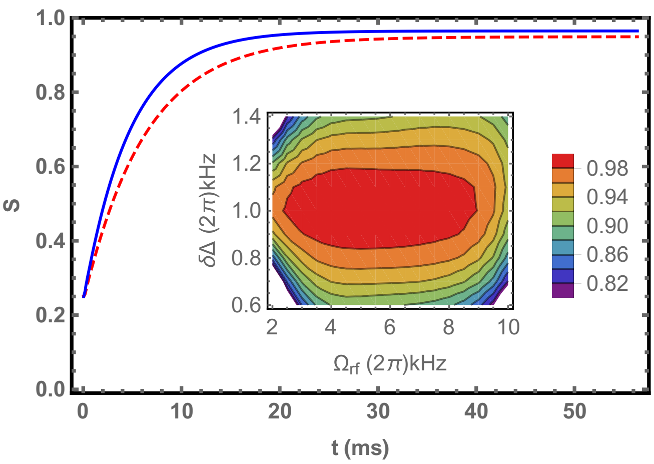

FIG. 3. Dissipative dynamic of the singlet state in a nuclear dimer (interacting with each other $g_{12} = (2\pi)4.2$ kHz) coupled to the NV spin $(a_{\parallel_1}, a_{\perp_1}) = (2\pi)(-6.39, 12.54)$ kHz and $(a_{\parallel_2}, a_{\perp_2}) = (2\pi)(-2.77, 12.67)$ kHz, which is governed by the original master equation and NV reset procedure. The initial state of nuclear pair is in a completely mixed state $\rho_n = I/4$ and NV spin is reinitialized to state $|-_x\rangle$ every 50 μs ($T_{1\rho} = 2$ ms). Adjusting the MW Rabi frequency allows us to have $\Delta_1 = (2\pi)(-0.10)$ kHz and $\Delta_2 = (2\pi)1.91$ kHz, with $\Omega_{\mathrm{rf}} = (2\pi)20$ kHz, and the singlet state is generated as shown by the blue line. As a comparison, we consider a small nuclear bath (the dashed red line), in which coupling strengths of three different nuclear spins are $(a_{\parallel_3}, a_{\perp_3}) = (2\pi)(-22.1, 20.0)$ kHz, $(a_{\parallel_4}, a_{\perp_4}) = (2\pi)(14.2, 6.4)$ kHz and $(a_{\parallel_5}, a_{\perp_5}) = (2\pi)(-17.8, 1.2)$ kHz. The inset shows the LN vs. Ω_{rf} and $\delta\Delta$ with the evolution time 30 ms.

where $g_{12} = \frac{\mu_0}{4\pi}\frac{\hbar\gamma_n^2}{r_{ij}^3}(1–3\cos^2\theta_{ij})$ is the coupling strength between nuclear spins, θ_{ij} is the angle between the nuclear spin position vector $\vec{r}_{ij}$ and the magnetic field. It is easy to see that $|S\rangle$ is an eigenstate of the last term in H'_T. Therefore, one can proceed analogously to the case of noninteracting nuclear spins and adjust the detunings and the Rabi frequency of the rf field to ensure that the singlet state is unique. Then the singlet state of the pair of interacting nuclear spins in a dimer is again generated as the steady state (see the simulation in Fig. 3). In this simulation we consider a ^{13}C dimer ($\sim$1.3 nm from NV center) in diamond, the NV position [0,0,0] nm and NV axis is parallel to the crystal axis [111]. The magnetic field is applied along NV axis. $d_{\mathrm{cc}} = 0.154$ nm is the C-C bond length. A value of $g_{12} = (2\pi)4.2$ kHz (or 1.37 kHz) indicates the dimer is either aligned along the direction of the external field B (or tilted from the magnetic field by 109.5°), which tends to have comparable perpendicular coupling components and small imbalanced parallel components. Suppose $g_{12} = (2\pi)4.2$ kHz, and nuclear spins positions as [0.625, −0.624, −0.803] nm and [0.536, −0.714, −0.893] nm, as shown in Fig. 3, a singlet pair with high LN 0.98 is generated. The scheme is robust to the fluctuation of the detunings and Rabi frequency of rf field; see Fig. 3. In general, there are many ^{13}C nuclear spins surrounding the NV spin. Therefore, we also performed simulations which consider the dimer in a small nuclear bath (three additional nuclear spins coupled to the NV spin). For 0.55% of ^{13}C spins abundance, the probability of finding the dimer along the NV axis within 1–1.5 nm of the NV center is $\sim$2.4% (see Appendix D).

V. CONCLUSIONS

Before concluding, we stress that the generation of a singlet state of nuclear spins in experiments by using unitary preparation is extremely difficult at room temperature. First, unitary preparation depends on the selective quantum operations between each nuclei and the NV center. If two nuclei have similar couplings to the NV center, no matter if they interact with each other or not, individually addressing one of them without affecting the other is quite challenging. Second, the NV center lifetime being several orders shorter than in Ref. [16], limits high fidelity quantum operations. Additionally, at least four two-qubit quantum gates are necessary for unitary preparation, each fidelity is smaller than 0.9 [11], which gives the fidelity 0.66 of a singlet state.

In summary, we propose a dissipative approach to generate long-lived singlet pair in both noninteracting and interacting nuclear spins which are dipole coupled to the electron spin of a nearby NV center in diamond at room temperature and ambient conditions. The key idea of our protocol is the combination of periodic resets of the electron spin which generates tunable dissipation and coherent radio-frequency control of the target nuclear spins. This combination stabilises the protocol against the impact of T_1 processes of the NV center and we show that dissipative entanglement is generated for any initial state of the spins and is robust in the presence of external field fluctuations and other imperfections. High-fidelity nuclear singlet states provide a resource for a host of applications.

ACKNOWLEDGMENTS

This work was supported by the ERC Synergy Grant BioQ and the EU projects DIADEMS, EQUAM, and HYPERDIAMOND, as well as DFG CRC/TRR21.

APPENDIX A: EFFECTIVE HAMILTONIAN OF THE SYSTEM

The Hamiltonian of the whole system is given by $H_{\mathrm{tot}} = H_e + H_n + H_{\mathrm{driv}} + H_{\mathrm{int}}$, in which H_e, H_n, and H_{driv} are the Hamiltonian of the NV center in diamond, of nuclear spins, and of the driving MW and rf field, respectively. And we have

$$\begin{aligned} H_e &= DS_z^2 + \gamma_e \vec{B}_0 \vec{S}, \\ H_n &= \sum_{i=1,2} \gamma_n \vec{B}_0 \vec{I}_i, \\ H_{\mathrm{driv}} &= \sqrt{2}\Omega_{\mathrm{mw}} \cos\omega_{\mathrm{mw}} t\, S_x + \sum_{i=1,2} 2\Omega_{\mathrm{rf}} \cos\omega_{\mathrm{rf}} t\, I_i^x, \\ H_{\mathrm{int}} &= \sum_{i=1,2} \left(\frac{\mu_0}{4\pi}\frac{\hbar\gamma_e\gamma_n}{r_i^3}\right)\left[\vec{S}\vec{I}_i - 3(\vec{S}\cdot\vec{e}_{r_i})(\vec{I}_i\cdot\vec{e}_{r_i})\right]. \end{aligned} \quad \text{(A1)}$$

Herein D denotes zero-field splitting of the electronic ground state, $\gamma_e = (2\pi)28$ GHz/T, γ_n the gyromagnetic ratio of the electron spin and nuclear spins, $\vec{S}$ the electron spin-1 vector operator, and $\vec{B}_0$ the magnetic field vector. Ω_{mw} (Ω_{rf}) is the Rabi frequency of the MW (rf) field with frequency ω_{mw}

($\omega_{\rm rf}$). r_i is the distance between the electron spin and nuclear spin and $\vec{e}_{r_i}$ presents unit direction vector connecting the two coupled spins involved.

Working in a frame that is rotating with the microwave frequency that is resonant with the electronic transition $m_s = 0$ and $m_s = -1$. Within the ground state, $m_s = 0$ and $m_s = -1$ manifold form a two-level system, for which the Hamiltonian is

$$H_{\rm intf} = \sum_{i=1,2} \left(\sigma_z^e + 1/2\right)\vec{A}_i \cdot \vec{I}_i, \tag{A2}$$

where

$$\vec{A}_i = \frac{g_0}{r_i^3}\left[3e_{ri}^z e_{r_i}^x, 3e_{ri}^z e_{r_i}^y, \left(3\left(e_{r_i}^z\right)^2 - 1\right)\right]$$

is the hyperfine coupling vector with $g_0 = \frac{-\mu_0\hbar\gamma_e\gamma_{n_i}}{4\pi}$. The direction of $\vec{I}_i$ is determined by the magnetic field unit vector $\vec{b} = [\theta,\phi] = [\sin\theta\cos\phi, \sin\theta\sin\phi, \cos\theta] = [b_x,b_y,b_z]$. $\sigma_z^e = \frac{1}{2}(|-1\rangle\langle-1| - |0\rangle\langle 0|)$. $\vec{A} = (a_{\parallel_i}, a_{\perp_i})$ with $a_{\parallel_i}$ and $a_{\perp_i}$ denotes the related coupling components parallel and perpendicular to the nuclear spin quantization axes $a_{\parallel i} = \vec{A}_i \cdot \vec{b}$ and $a_{\perp i} = \sqrt{|\vec{A}_i|^2 - a_{\perp i}^2}$. The coupling vector $\vec{A} = (a_{\parallel_i}, a_{\perp_i})$ is adjustable by the magnetic field direction. One can shift the magnetic field direction to have $a_{\perp i} = a_{\perp j}$ for these two nuclear spins and $a_{\parallel i} \neq a_{\parallel j}$, which satisfies the requirement for singlet generation of two noninteracting nuclear spins near the NV center.

We can rewrite the effective Hamiltonian of the NV spin as $H_{\rm NV} = \Omega_{\rm mw}\sigma_z$, with eigenstates $\{|+_x\rangle = \frac{1}{\sqrt{2}}(|0\rangle + |-1\rangle), |-_x\rangle = \frac{1}{\sqrt{2}}(|0\rangle - |-1\rangle)\}$ microwave dressed states and $\sigma_z = \frac{1}{2}(|+_x\rangle\langle +_x| - |-_x\rangle\langle -_x|$. Consider the simplified Hamiltonian of system as

$$H'_{\rm tot} = \Omega_{\rm mw}\sigma_z + \sum_{i=1,2} 2\Omega_{\rm rf}\cos\omega_{\rm rf}t\, I_i^x + \left(\gamma_n B_0 + \frac{a_{\parallel i}}{2}\right) I_i^z + \sigma_x\left(a_{\parallel_i} I_i^z + a_{\perp i} I_i^{\hat{x}}\right). \tag{A3}$$

Working in a rotating frame with $H_0 = \Omega_{\rm mw}\sigma_z + \sum_{i=0}^{2}\omega_{\rm rf} I_i^z$ and $a_{\parallel_i}, a_{\perp_i} \ll \Omega_{\rm mw}, \omega_{\rm rf}$, rotation wave approximation gives

$$H''_{\rm tot} = \sum_{i=1,2} \Omega_{\rm rf} I_i^x + \Delta_i I_i^z + \frac{a_{\perp_i}}{4}(\sigma_- I_i^+ + \sigma_+ I_i^-), \tag{A4}$$

in which $\Delta_i = (\gamma_n B_0 + \frac{a_{\parallel i}}{2}) - \omega_{\rm rf}$ and $\omega_{\rm rf} = \Omega_{\rm mw}$.

We employ the Lindblad master equation to investigate the dynamics of the whole system described by density matrix ρ. This is described by

$$\frac{d}{dt}\rho = -i[H''_{\rm tot}, \rho] + \mathcal{D}_e[L]\rho, \tag{A5}$$

in which $\mathcal{D}_e[c]\rho = c\rho c^\dagger - \frac{1}{2}\{c^\dagger c, \rho\}$ and $L = \sqrt{\Gamma_N}|-_x\rangle\langle +_x|$ with the effective dissipation of the electron spin Γ_N. Here the reset of the NV to the state $|-_x\rangle$ every $t_{\rm re}$ introduces an effective interaction time in each cycle, which results in another effective relaxation mechanism of the electron. Therefore, the effective relaxation of the NV spin includes two parts: the lifetime and the reset of the electron spin $\Gamma_N = 1/T_{1\rho} + 1/t_{\rm re}$. Additionally, in our scheme frequent resets of NV spin into the state $|-_x\rangle$ with $t_{\rm re} \ll T_{1\rho}$ ensures electron spin state stays in state $|-_x\rangle$ and $\Gamma_N \approx 1/t_{\rm re}$.

APPENDIX B: ADIABATIC ELIMINATION OF ELECTRONIC DEGREES OF FREEDOM

Because the coupling strengths between the electron spin and nuclear spins are small compared to the energy scales of electron and nuclear spins, perturbation theory allows us to derive the effective master equation for the nuclear spin subspace. When electron spin state stays in state $|-_x\rangle$, the flip-flop of transition $|\uparrow -_x \downarrow\rangle \leftrightarrow |\downarrow -_x \uparrow\rangle$ is mediated by $|m\rangle = |\downarrow +_x \downarrow\rangle$. Adiabatic elimination of the state $|m\rangle$ we reduce the dynamics to an effective master equation involving ground $\{|g_1\rangle, |g_2\rangle\} = \{|\uparrow -_x \downarrow\rangle, |\downarrow -_x \uparrow\rangle\}$ manifold [38],

$$\frac{d}{dt}\rho_{\rm eff} = -[H_T, \rho_{\rm eff}] + \mathcal{D}[L_{\rm eff}]\rho_{\rm eff}, \tag{B1}$$

in which effective Hamilton and Lindblad operators

$$\begin{aligned} H_T &= V^\dagger\left[H_0^{-1} + \left(H_0^{-1}\right)^\dagger\right]V + H_g, \\ L_{\rm eff} &= L_i H_0^{-1} V, \end{aligned} \tag{B2}$$

connecting only ground states in $\{|\uparrow -_x \downarrow\rangle, |\downarrow -_x \uparrow\rangle\}$. Here, V are the perturbative excitations from the ground states in to the mediate state $|\downarrow +_x \downarrow\rangle$. H_g is the Hamiltonian for ground states, and

$$H_0 = H_m - \sum_i \frac{i}{2} L_i L_i^\dagger,$$

with H_m for the mediate state. Therefore, one has Linblad operators as

$$\begin{aligned} L_1 &= \sqrt{\Gamma_N}|g_1\rangle\langle m|, \\ L_2 &= \sqrt{\Gamma_N}|g_2\rangle\langle m|. \end{aligned} \tag{B3}$$

The non-Hermitian Hamiltonian can be divided into two parts, denoted by the initial state of the exciting field

$$\begin{aligned} H_0^{(1)} &= \Delta_1 - \frac{i\Gamma_N}{2}|m\rangle\langle m|, \\ H_0^{(2)} &= \Delta_2 - \frac{i\Gamma_N}{2}|m\rangle\langle m|. \end{aligned} \tag{B4}$$

And V is determined by the interaction Hamiltonian $\frac{a_{\perp i}}{4}(\sigma_- I_i^+ + \sigma_+ I_i^-)$.

Because the NV is kept in state $|-_x\rangle$, the dynamic of the NV is eliminated and we have effective master equation

$$\frac{d}{dt}\rho_n = -i[H_T, \rho_n] + \sum_{i=1,2}\mathcal{D}[M_i]\rho_n + \mathcal{D}[L]\rho_n, \tag{B5}$$

in which the intrinsic dissipations of nuclear spins are included as the second item, $M_i = \sqrt{\Gamma_i} I_i^-$ with Γ_i the dephasing rate of the nuclear spins. Effective dissipation induced by the electron reset is given as $L = \sum_i \alpha_i I_i^-$ with $\alpha_j = \frac{\sqrt{\Gamma_N}a_{\perp j}/4}{-\Delta_j + i\Gamma_N/2}$. And the effective Hamiltonian is

$$H_T = \sum_{i=1,2} \Omega_{\rm rf} I_i^x + \Delta_i I_i^z. \tag{B6}$$

APPENDIX C: NUCLEAR COHERENCE AND DEPOLARIZATION INDUCED BY LASER ILLUMINATION

In this part, we will use the spin-fluctuator model [36] to obtain the dephasing and depolarization rates of the nuclear spin under green illumination which leads to the NV reset. Consider the nuclear spin and the NV spin environment under green illumination, we have the Hamiltonian as

$$H_{\mathrm{ni}} = \gamma_{\mathrm{ni}} B_0 I_i^z + S_z\left(a_{\parallel_i} I_i^z + \frac{a_{\perp_i}}{2} I_i^+ + \mathrm{H.c.}\right). \quad \text{(C1)}$$

In the simple model we assume that under strong green illumination the NV spin projection fluctuates by $\pm\frac{1}{2}$ about its average so that we can rewrite the Hamiltonian as

$$H'_{\mathrm{ni}} = \gamma_{\mathrm{ni}} B_0 I_i^z + f_{\mathrm{opt}}(t)\left(a_{\parallel_i} I_i^z + \frac{a_{\perp_i}}{2} I_i^+ + \mathrm{H.c.}\right), \quad \text{(C2)}$$

in which $f_{\mathrm{opt}}(t) = \{-\frac{1}{2},\frac{1}{2}\}$ described a Bernoulli process, assuming $\langle f_{\mathrm{opt}}(t)\rangle = 0$ and correlation function $\langle f_{\mathrm{opt}}(t) f_{\mathrm{opt}}(0)\rangle = \langle f_{\mathrm{opt}}^2(0)\rangle e^{-2\Gamma_{\mathrm{illum}}|t|} = \frac{1}{4}e^{-2\Gamma_{\mathrm{illum}}|t|}$. Γ_{illum} is the forward and backward effective transition rate controlled by the laser intensity.

The nuclear spin dephasing rate is induced by the term $f_{\mathrm{opt}}(t) a_{\parallel_i} I_i^z$, while the depolarization rate is related to the term $f_{\mathrm{opt}}(t)(\frac{a_{\perp_i}}{2} I_i^+ + \mathrm{H.c.})$. Therefore, dephasing and depolarization of the nuclear spin are given by $\frac{a_{\parallel_i}^2}{8\Gamma_{\mathrm{illum}}}$ and $\frac{a_{\perp_i}^2}{(\gamma_{\mathrm{ni}} B/2)^2+\Gamma_{\mathrm{illum}}}\frac{\Gamma_{\mathrm{illum}}}{8}$, respectively. Consider the NV initialization requires time $\tau = 1\ \mu$s, and every $t_{\mathrm{re}} = 40\ \mu$s we reset NV spin, the dephasing and depolarization of the nuclear spin caused by green illumination are given as $1/T_{\mathrm{opt1}} = \frac{a_{\perp_i}^2}{(\gamma_{\mathrm{ni}} B/2)^2+\Gamma_{\mathrm{illum}}}\frac{\Gamma_{\mathrm{illum}}\tau}{8t_{\mathrm{re}}}$, and $1/T_{\mathrm{opt2}} = \frac{a_{\parallel_i}^2}{\Gamma_{\mathrm{illum}}}\frac{\tau}{8t_{\mathrm{re}}}$, respectively. Suppose $a_{\parallel_i} < 10$ kHz and $\Gamma_{\mathrm{illum}} \sim 400$ kHz [36], $\tau \gg t_{\mathrm{re}}$ and $a_{\perp_i} \gg \gamma_{\mathrm{ni}} B$ induce the effect from the green illumination negligible.

APPENDIX D: INHOMOGENEITIES INTRODUCED BY THE DRIVING FIELDS

In order to account for inhomogeneities introduced by the driving fields during the cycles, we have the fluctuating terms in the stochastic Hamiltonian as

$$H_T = \sum_{i=1,2} \Omega_{\mathrm{rf}} I_i^x + \Delta_i I_i^z + B_\Omega(t) I_i^x + B_\Delta(t) I_i^z, \quad \text{(D1)}$$

where $B_\Omega(t)$ and $B_\Delta(t)$ are the random processes describing the fluctuating frequencies. After each consecutive cycle, we include random $B_\Omega(m t_{\mathrm{re}}) = B_\Omega n$ and $B_\Delta(m t_{\mathrm{re}}) = B_\Delta n$ with m natural number and n is a zero-mean unit-variance gaussian random variable, which is time uncorrelated. By considering the particular time-dependence of these stochastic processes, we numerically integrate the noisy dynamics. This allows us to study the effects of inhomogeneities introduced by the driving fields on the singlet generation. The presence of frequencies noise is given and it is shown that our scheme is robust to the fluctuations of the driving field; see Fig. 4.

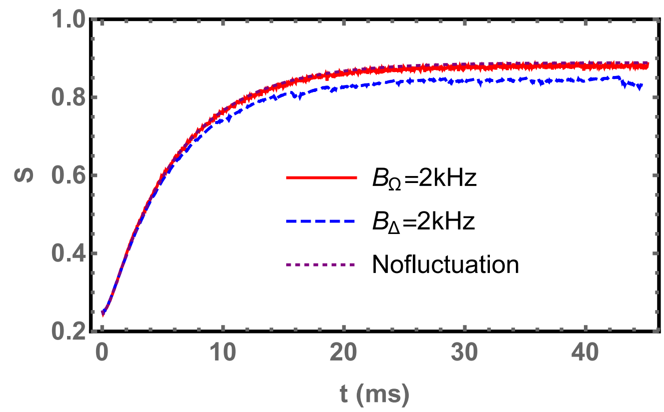

FIG. 4. The population evolutions of the singlet and three triplet states $|S\rangle = \frac{1}{\sqrt{2}}(|\uparrow_1\downarrow_2\rangle - |\downarrow_1\uparrow_2\rangle)$ as a function of time for a fully mixture state $\rho_n = I/4$ initially. The two nuclei are coupled to the NV center and $\Delta = (2\pi)4$ kHz, $\Omega_{\mathrm{rf}} = (2\pi)16$ kHz, the parameters of the purple dashed line in Fig. 2(d) is the same in Fig. 2(d). The presence of frequencies noise are given and it is shown that our scheme is robust to the fluctuations of the driving field, $B_\Omega = B_\Delta = 2$ kHz.

APPENDIX E: PROBABILITY FOR FINDING A ^{13}C DIMER

Here we calculate the probability to find a dimer appearing within 1–1.5 nm of the NV center. Natural abundance ^{13}C spins $C_c = 1.1\%$ gives a probability of a site at distance R from NV spin $P_C = \exp(-C_c N_R)$ with $N_R = 16\frac{4\pi R^3}{3V_c}$ the total carbon sites and $V_c = 0.0454$ nm^3 is the volume of a unit cell. Therefore, one can have the probability of the first dimer on the shell (thickness ΔR) from NV spin as $\Delta P = \exp(-C_c^2 N_R) - \exp(-C_c^2 N_{R+\Delta R})$. In diamond of natural abundance, there is ∼29% probability to have at least one nuclear dimer appearing within 1–1.5 nm (the possible range) from the NV center. The probability of finding the dimer parallel the NV axis is about 7.3%. Also a half natural abundance gives a probability of finding the dimer along the NV axis ∼2.4%.

[1] W. S. Warren, E. Jenista, R. T. Branca, and X. Chen, Increasing hyperpolarized spin lifetimes through true singlet eigenstates, Science **323**, 1711 (2009).

[2] P. Vasos, A. Comment, R. Sarkar, P. Ahuja, S. Jannin, J.-P. Ansermet, J. Konter, P. Hautle, B. van den Brandt, and G. Bodenhausen, Long-lived states to sustain hyperpolarized magnetization, Proc. Natl. Acad. Sci. USA **106**, 18469 (2009).

[3] G. Pileio and M. H. Levitt, J-stabilization of singlet states in the solution NMR of multiple-spin systems, J. Magn. Reson. **187**, 141 (2007).

[4] G. Pileio, M. Carravetta, and M. H. Levitt, Extremely Low-Frequency Spectroscopy in Low-Field Nuclear Magnetic Resonance, Phys. Rev. Lett. **103**, 083002 (2009).

[5] A. Bornet, P. Ahuja, R. Sarkar, L. Fernandes, S. Hadji, S. Y. Lee, A. Haririnia, D. Fushman, G. Bodenhausen, and P. R. Vasos, Long-lived states to monitor protein unfolding by proton NMR, Chem. Phys. Chem. **12**, 2729 (2011).

[6] P. Ahuja, R. Sarkar, P. R. Vasos, and G. Bodenhausen, Diffusion coefficients of biomolecules using long-lived spin states, J. Am. Chem. Soc. **131**, 7498 (2009).

[7] A. Reiserer, N. Kalb, M. S. Blok, K. J. M. van Bemmelen, T. H. Taminiau, R. Hanson, D. J. Twitchen, and M. Markham, Robust Quantum-Network Memory Using Decoherence-Protected Subspaces of Nuclear Spins, Phys. Rev. X **6**, 021040 (2016).

[8] S. J. DeVience, R. L. Walsworth, and M. S. Rosen, Preparation of Nuclear Spin Singlet States Using Spin-Lock Induced Crossing, Phys. Rev. Lett. **111**, 173002 (2013).

[9] M. Emondts, M. P. Ledbetter, S. Pustelny, T. Theis, B. Patton, J. W. Blanchard, M. C. Butler, D. Budker, and A. Pines, Long-Lived Heteronuclear Spin-Singlet States in Liquids at a Zero Magnetic Field, Phys. Rev. Lett. **112**, 077601 (2014).

[10] Y. Wu, F. Jelezko, M. B. Plenio, and T. Weil, Diamond quantum devices in biology, Angew. Chem., Int. Ed. **55**, 6586 (2016).

[11] T. H. Taminiau, J. Cramer, T. van der Sar, V. V. Dobrovitski, and R. Hanson, Universal control and error correction in multi-qubit spin registers in diamond, Nat. Nanotechnol. **9**, 171 (2014).

[12] G. Waldherr, Y. Wang, S. Zaiser, M. Jamali, T. Schulte-Herbrüggen, H. Abe, T. Ohshima, J. Isoya, J. Du, P. Neumann *et al.*, Quantum error correction in a solid-state hybrid spin register, Nature **506**, 204 (2014).

[13] G. A. Álvarez, C. O. Bretschneider, R. Fischer, P. London, H. Kanda, S. Onoda, J. Isoya, D. Gershoni, and L. Frydman, Local and bulk 13c hyperpolarization in nitrogen-vacancy-centred diamonds at variable fields and orientations, Nat. Commun. **6**, 8456 (2015).

[14] Q. Chen, I. Schwarz, F. Jelezko, A. Retzker, and M. B. Plenio, Optical hyperpolarization of ^{13}C nuclear spins in nanodiamond ensembles, Phys. Rev. B **92**, 184420 (2015).

[15] J. Scheuer, I. Schwartz, Q. Chen, D. Schulze-Sünninghausen, P. Carl, P. Höfer, A. Retzker, H. Sumiya, J. Isoya, B. Luy *et al.*, Optically induced dynamic nuclear spin polarization in diamond, New J. Phys. **18**, 013040 (2016).

[16] A. Jarmola, V. M. Acosta, K. Jensen *et al.*, Temperature-and Magnetic-Field-Dependent Longitudinal Spin Relaxation in Nitrogen-Vacancy Ensembles in Diamond, Phys. Rev. Lett. **108**, 197601 (2012).

[17] M. B. Plenio, S. F. Huelga, A. Beige, and P. L. Knight, Cavity-loss-induced generation of entangled atoms, Phys. Rev. A **59**, 2468 (1999).

[18] M. B. Plenio and S. F. Huelga, Entangled Light from White Noise, Phys. Rev. Lett. **88**, 197901 (2002).

[19] C. A. Muschik, E. S. Polzik, and J. I. Cirac, Dissipatively driven entanglement of two macroscopic atomic ensembles, Phys. Rev. A **83**, 052312 (2011).

[20] M. J. Kastoryano, F. Reiter, and A. S. Sørensen, Dissipative Preparation of Entanglement in Optical Cavities, Phys. Rev. Lett. **106**, 090502 (2011).

[21] D. D. B. Rao and K. Mølmer, Dark Entangled Steady States of Interacting Rydberg Atoms, Phys. Rev. Lett. **111**, 033606 (2013).

[22] D. D. B. Rao, S. Yang, and J. Wrachtrup, Dissipative entanglement of solid-state spins in diamond, Phys. Rev. A **95**, 022310 (2017).

[23] J. N. Greiner, D. D. B. Rao, and J. Wrachtrup, Purification of an unpolarized spin ensemble into entangled singlet pairs, Sci. Rep. **7**, 529 (2017).

[24] T. Ramos, H. Pichler, A. J. Daley, and P. Zoller, Quantum Spin Dimers from Chiral Dissipation in Cold-Atom Chains, Phys. Rev. Lett. **113**, 237203 (2014).

[25] Q. Chen, I. Schwarz, and M. B. Plenio, Dissipatively stabilized quantum sensor based on indirect nuclear-nuclear interactions, arXiv:1702.05144 [Phys. Rev. Lett. (to be published)].

[26] A. Bermudez, T. Schaetz, and M. B. Plenio, Dissipation-Assisted Quantum Information Processing with Trapped Ions, Phys. Rev. Lett. **110**, 110502 (2013).

[27] H. Krauter, C. A. Muschik, K. Jensen, W. Wasilewski, J. M. Petersen, J. I. Cirac, and E. S. Polzik, Entanglement Generated by Dissipation and Steady State Entanglement of Two Macroscopic Objects, Phys. Rev. Lett. **107**, 080503 (2011).

[28] Y. Lin, J. Gaebler, F. Reiter, T. Tan, R. Bowler, A. Sørensen, D. Leibfried, and D. Wineland, Dissipative production of a maximally entangled steady state of two quantum bits, Nature **504**, 415 (2013).

[29] S. Shankar, M. Hatridge, Z. Leghtas, K. Sliwa, A. Narla, U. Vool, S. M. Girvin, L. Frunzio, M. Mirrahimi, and M. H. Devoret, Autonomously stabilized entanglement between two superconducting quantum bits, Nature **504**, 419 (2013).

[30] H. Christ, J. I. Cirac, and G. Giedke, Quantum description of nuclear spin cooling in a quantum dot, Phys. Rev. B **75**, 155324 (2007).

[31] P. London, J. Scheuer, J.-M. Cai, I. Schwarz, A. Retzker, M. B. Plenio, M. Katagiri, T. Teraji, S. Koizumi, J. Isoya *et al.*, Detecting and Polarizing Nuclear Spins with Double Resonance on a Single Electron Spin, Phys. Rev. Lett. **111**, 067601 (2013).

[32] M. B. Plenio, Logarithmic Negativity: A Full Entanglement Monotone That is not Convex, Phys. Rev. Lett. **95**, 090503 (2005).

[33] $\mathrm{LN}(\rho_{\mathrm{ss}}) = \log_2 ||\rho_{\mathrm{ss}}^{\mathrm{PT}}||_1$ is a measure of entanglement, where $||\cdot||_1$ denotes the trace norm and $\rho_{\mathrm{ss}}^{\mathrm{PT}}$ is the partial transpose operation appled to ρ_{ss} corresponding to steady state $|\psi_{\mathrm{ss}}\rangle$.

[34] G. Waldherr, J. Beck, M. Steiner, P. Neumann, A. Gali, T. Frauenheim, F. Jelezko, and J. Wrachtrup, Dark States of Single Nitrogen-Vacancy Centers in Diamond Unraveled by Single Shot NMR, Phys. Rev. Lett. **106**, 157601 (2011).

[35] M. Grinolds, P. Maletinsky, S. Hong, M. Lukin, R. Walsworth, and A. Yacoby, Quantum control of proximal spins using nanoscale magnetic resonance imaging, Nat. Phys. **7**, 687 (2011).

[36] P. C. Maurer, G. Kucsko, C. Latta, L. Jiang, N. Y. Yao, S. D. Bennett, F. Pastawski, D. Hunger, N. Chisholm, M. Markham *et al.*, Room-temperature quantum bit memory exceeding one second, Science **336**, 1283 (2012).

[37] W. K. Wootters, Entanglement of Formation of an Arbitrary State of Two Qubits, Phys. Rev. Lett. **80**, 2245 (1998).

[38] F. Reiter and A. S. Sørensen, Effective operator formalism for open quantum systems, Phys. Rev. A **85**, 032111 (2012).